Predictive Health Status Assessment of a Launch Vehicle Engine in an Ascending Flight Based on Vibration Signals

ZHIGUO ZHOU [ID], Member, IEEE
LIJING HUANG [ID]
Beijing Institute of Technology, Beijing, China

RULIANG LIN [ID]
Beijing Institute of Technology, Beijing, China
Beijing Aerospace Wanyuan Science and Technology Company, Ltd, Beijing, China

The launch vehicle engine is a typical fuzzy environment in which the health status is extremely difficult to analyze. Current prognostics and health management (PHM) research on rocket engines is almost always a study of real-time health conditions, lacking a significant reference for risk prevention. Moreover, the current evaluation methods are inadequate in terms of universality and are too dependent on expert experience. Our work is the first to propose a multilevel and multifactor predictive evaluation method for the health status assessment of launch vehicle engines. The hierarchy of health assessment is divided by a data-driven method, and the health status of a rocket engine is evaluated based on a prediction algorithm and a fuzzy comprehensive evaluation method. The minimum evaluation error is 0.24% when the method is validated with measured data from long-range launch vehicle engines, which shows that the method presented in this article has a good effect on the prediction and evaluation of launch vehicle engines.

I. INTRODUCTION

Launch vehicles can cause several types of vibrations due to intense thrust pulses and aerodynamic mutations during launch and flight. A vibration signal comprises low, medium, and high frequencies, which seriously affects the equipment structure and electrical system of multiple systems in a rocket. For example, physical movement may become difficult and decision-making may become chaotic when astronauts are exposed to low-frequency vibrations, which can easily lead to the failure of rocket launch missions and casualties [1]. Optimizing the material and structure of a rocket and analyzing the state of the rocket using information science methods are the main ways to reduce vibration generation and damage. As shown in Fig. 1, health assessment technology is an important part of the rocket adaptive fault tolerance technology process. Research from the perspective of information science is designed to provide early information on fault tolerance for potential failures. Rocket health preassessments are more meaningful for real space missions.

A launch vehicle engine is a typical fuzzy environment [2], and its internal mechanism cannot be explored be relying solely on artificial intelligence (AI) and computational science. For industrial and military equipment, prognostics and health management (PHM) studies for a system are much more difficult than fault detection for a single component. The authors in [3], [4], and [5] proposed self-organizing and self-evolving fuzzy neural networks for different fuzzy systems. However, this approach is very susceptible to anomalous data that can lead to erroneous results. For launch vehicle fuzzy systems, each launch may be for a different model of a rocket, and the same model of a rocket may also have different types of components. The results of the above methods are difficult to obtain through practical verification. Rocket engine testing can summarize a large number of failure modes and human experience, thus accurately reflecting real-life scenarios. It also reduces the impact of anomalous data on the results.

Researchers have developed various methods for rocket engine PHM, and the current methods can be categorized into three types [6]:

1) Model-based methods.
2) Expert-experience-based methods.
3) Data-driven methods.

Researchers have conducted extensive research on the identification and evaluation of rocket engine faults.

The basic principle of a mathematical model for engine PHM is to treat the output of the engine mathematical model as a standard state and determine the deviation degree of the actual working state of the engine from the standard state through various indicators. If the deviation degree is too large, the engine working conditions in this state are regarded as abnormal. Model-based methods can be divided into two types: analytical models and system identification. Based on an analytical model, Davidson et al. [7] designed a linear engine model for the Advanced Health Management
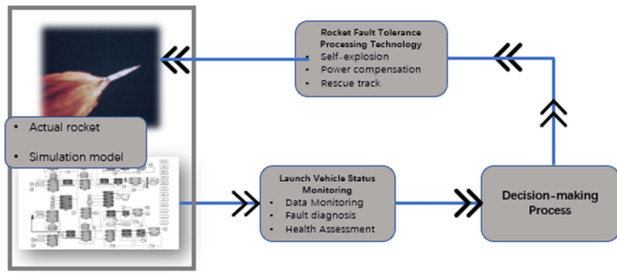
Fig. 1.   Rocket adaptive fault tolerance technology.

System (AHMS) using a threshold to achieve online engine anomaly detection. Breedveld [8] compared the effects of continuous state estimation and discrete state estimation for space shuttle main engine (SSME) fault diagnosis and showed that discrete state estimation performs best when the measurement noise is negligible. Continuous state estimation is used when measurement noise is present. Based on a system identification model, Srivastava et al. established a correspondence between the spectral intensity of SSME plume characteristics and engine performance parameters through neural network training, and based on this relationship, the condition monitoring of an SSME was carried out [9]. In the 1990s, the United Technologies Research Center used the autoregressive moving average (ARMA) algorithm to monitor the steady-state process of SSMEs in real time when designing SSME HMSs [10]. Model-based approaches focus on how well they fit fuzzy systems, and one model cannot be adapted to different engines. Therefore, model-based approaches lack versatility.

The conventional method is based on expert systems for the problem of vibration failure of launch vehicle engines. However, with the development of technology and artificial intelligence, Big Data mining has proven to be an important and effective method [11]. Engle et al. developed an expert system-based inference mechanism, the prelaunch experiment system, for the preparation stage of an SSME during ignition, which facilitates the analysis of the overall health of a system by ground personnel [12]. Kurien et al. [13] experimented with health management techniques in the Deep Space One project from 1998 to 2001. Rockdyne et al. developed an expert system for turbopump fault diagnosis. This system contains both shallow and deep knowledge. Shallow knowledge refers to the experience and processes summarized by domain experts in analyzing and processing test data, and deep knowledge refers to any analytical model that can characterize the operating characteristics of engine turbopumps [14]. However, relying heavily on an expert system leads to subjective experience domination [15]. Nevertheless, there are three main problems with the use of manual analysis:

1) Personal cognitive limitations, i.e., the knowledge that each person has is limited.
2) An inefficient diagnosis requires considerable time and human resources.

3) A manual system can only be used for offline diagnosis and cannot meet the needs of online fault diagnosis [6].

Data-driven-based methods can be further subdivided into two types: statistical analysis and pattern recognition. Aiswarya et al. manually extracted the time and frequency domain features of a liquid rocket engine (LRE) running signal, used support vector machines to classify these features, and achieved 100% classification accuracy [16]. Wu et al. proposed a fault detection method with particle swarm optimization and a least squares support vector machine to improve the performance of an LRE [17]. Wang et al. proposed a deep separable convolutional neural network to predict the remaining useful life of aeroengines with monitoring data from different sensors [18]. Miao et al. proposed dual-task deep long short-term memory (LSTM) networks to unify the task of degradation evaluation and remaining useful life prediction of aeroengines [19]. Xu et al. used the quantum genetic algorithm to optimize a backpropagation (BP) neural network, train the BP neural network to generate two outputs, and perform fault diagnosis on an LRE [15]. The PHM approach based on digital twins is a deep combination of traditional PHM technology and digital twin technology. Mapping physical devices and virtual devices leverages data and model simulation technologies, which can realize the early prediction and accurate location of faults [20]. Among data-driven approaches, deep learning methods exhibit excellent adaptability and accuracy. A launch vehicle has a limited number of launches. The characteristics of a launch vehicle include few failure samples and a relative lack of historical experience. The limited fault data are not sufficient to support the training of a neural network. Thus, an accurate fault model cannot be obtained, and it is difficult to achieve fault location. Moreover, real data are susceptible to data scarcity, and simulation data are susceptible to the model accuracy.

In this article, based on the real-time data of a launch vehicle, a multilayer weight generation of the overall system is realized according to the expert score. At the same time, a deep neural network is used to predict future vibration signal trends, and the deviation between the actual data, the prediction data and the ideal state are calculated to obtain the actual and predicted health evaluation matrix. The evaluation and weight sets are used as input, and the health value of the top-level target is obtained through a comprehensive fuzzy assessment. This approach has important guiding significance for risk prevention of the ascending section of a rocket engine. Introducing expert experience to data-driven methods can solve the problem of the lack of data and low model accuracy. Using a modular approach, the health assessment of different objects can be achieved by replacing the prediction data and weight relationship. While improving the evaluation accuracy, the use of automated AI technology reduces economic expenses.
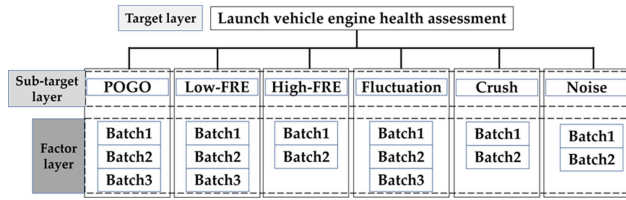
Fig. 2. Three-layer dataset structure.

Fig. 3. Predictive evaluation process.

II. ROCKET ENGINE HEALTH ASSESSMENT SYSTEM ARCHITECTURE

A. Data Hierarchy and Structure

The vibration signals for launch vehicle engines mainly include the following six categories: pogo vibration, low-frequency vibration, high-frequency vibration, fluctuation, shock signal, and noise. Pogo vibration refers to the pressure generated by multiple rocket engines during flight and the periodic vibrations generated by the external structure of the rocket, which can easily lead to pressure loss of control in the internal pipeline and instrument damage [21]. At the same time, when a rocket is flying at a high Mach speed, due to strong collisions between the rocket structure boundary and the external gas environment, a strong pulsating pressure will be produced, which will easily cause further equipment vibrations [22]. In the process of firing, several rocket engines begin to work, there is a sharp increase in the acceleration of the rocket, there will be low- and high-frequency signals and shock signals in the thrust system, and there is widespread noise when a large amount of mechanical equipment is working.

The vibration data used in this article are derived from measured data from the Long March series of carrier rocket engines, as shown in Fig. 2. The data include six types of vibration signals, including pogo vibration, low-frequency vibration, high-frequency vibration, fluctuation, shock, and noise. Each signal is divided into multiple groups of signal sensor batches, the data of the same batch are collected in the same acquisition sequence, and the test conditions are consistent. The system studied in this article is divided into three layers: the target layer, the subtarget layer, and the factor layer, which is convenient for the unified quantification of the health value of multiple influencing factors between the same level, and it is also easy to import weights.

According to historical experience, the impact of the six types of vibrations is different for the health state of the launch vehicle engine, and the degree of influence of the data collected by different types of sensors of the same type is also slightly different. The influence size relationship between the factors can be considered to simulate the data and obtain the health status value of a multilevel and multifactor system more accurately.

The amount of data accumulated by a launch vehicle is very large, and the use of sampling to reduce the amount of data and algorithm prediction with short-term data can significantly reduce the algorithm training time, reduce the
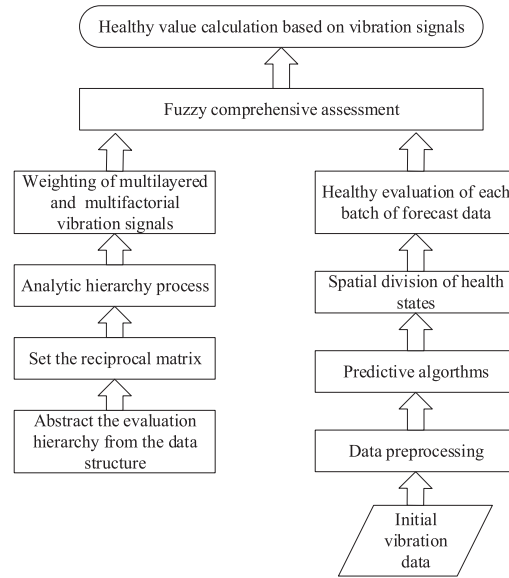
time cost of the overall process, and achieve the effect of predictive evaluation.

B. Architecture Process Evaluation

The comprehensive assessment process is shown in Fig. 3.

The overall process includes five main modules: data prediction, evaluation set generation, weight analysis, weight set generation, and fuzzy comprehensive evaluation. A modular structure is reasonable for the subsequent addition of evaluation levels and factors.

III. VIBRATION SIGNAL TREND PREDICTION

At present, most of the research on the state of a spacecraft such as a launch vehicle is concentrated in the real-time state. After data preprocessing, data measurement, anomaly detection, and other steps are performed to complete the real-time status assessment. However, there is a large delay in real-time status assessments, and they are of limited reference value to ground monitoring personnel. The rapid development of AI technology has greatly improved the efficiency and accuracy of data mining. Compared with that of the real-time status assessment mentioned above, the evaluation of the status of a launch vehicle engine based on prediction data is of more guiding significance for risk prevention and early warning.

A. Generic Step Prediction

The general forecasting process is divided into the following three steps:

1) Data preprocessing: The original vibration data of the launch vehicle are cleaned.
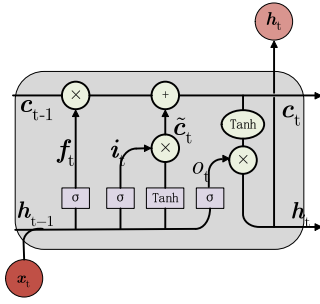2) Model training: The models are trained with data.
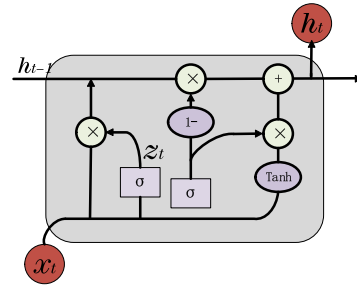
Fig. 4. LSTM network framework.

Fig. 5. GRU network framework.

3) Model prediction and error calculation: The data waveform is predicted, the data are saved, and the error values of the prediction, including the root mean square error (RMSE), coefficient of determination (R2), and mean absolute percentage error (MAPE), are calculated.

The RMSE formula is

$$\text{RMSE} = \sqrt{\frac{1}{N} \sum_{i=1}^{n} (Y_i - f(x_i))^2}. \tag{1}$$

The MAPE formula is

$$\text{MAPE} = \frac{100\%}{N} \sum_{i=1}^{n} \left| \frac{(Y_i - f(x_i))}{Y_i} \right|. \tag{2}$$

The R2 formula is

$$R^2 = 1 - \frac{\sum_i (Y_i - f(x_i))^2}{\sum_i (\bar{Y}_i - f(x_i))^2} \tag{3}$$

where Y_i represents each acquisition value in the test data, $f(x_i)$ represents each collection point in the prediction data, N represents the total number of collection points, and $\bar{Y}_i$ represents the average of the real data.

B. Predictive Models

1) LSTM Model: The LSTM model is expanded by a recurrent neural network (RNN) model. Since a launch vehicle is tested under a variety of vibration conditions, the collected data dynamically change. The sequential correlation of the signal data is the key to trend prediction. The LSTM model improves the prediction ability for long-term data compared with that of the RNN model and solves the gradient explosion and gradient disappearance problems in the data training process of the RNN model. At the same time, LSTM is more stable for actual project landing [23], [24]. Fig. 4 shows the model structure of the LSTM network:

Forget gate function

$$f_t = \sigma(W_f \cdot (h_{t-1}, x_t) + b_f). \tag{4}$$

Input gate function

$$i_t = \sigma(W_i \cdot (h_{t-1}, x_t) + b_i). \tag{5}$$

Candidate vector

$$\tilde{c}_t = \tanh(W_c g(h_{t-1}, x_t) + b_c). \tag{6}$$

State update after combining candidate vectors

$$c_t = f_t * c_{t-1} + i_t * \tilde{c}_t. \tag{7}$$

Filtered output function

$$o_t = \sigma(W_o \cdot (h_{t-1}, x_t) + b_o) \tag{8}$$

$$h_t = o_t * \tanh(c_t). \tag{9}$$

2) GRU Model: A gated recurrent unit (GRU) is a very effective variant of the LSTM network. A GRU network is simpler than an LSTM network and is very popular at present. It can also solve the problem of long dependence in RNNs [25].

In LSTM, three gate functions are introduced: an input gate, a forget gate, and an output gate. However, in GRU model, there are only two gates: an update gate and a reset gate. The structure of the model is shown in Fig. 5:

3) Weighted Moving Average: The moving average (MA) is a common tool used in technical analysis to analyze time series. Common moving averages include the simple moving average (SMA), weighted moving average (WMA), and exponential moving average (EMA) [26]. The SMA algorithm formula is expressed as follows:

$$Ft = \frac{(A_{t-1} + A_{t-2} + A_{t-3} + \ldots + A_{t-n})}{n} \tag{10}$$

where Ft is the predicted value for the next period, n is the number of periods of the MA, A_{t-1} is the previous actual value, and A_{t-2}, A_{t-3}, and A_{t-n} represent the actual values of the first two periods and the first three periods up to the first N periods.

The WMA model is shown in the following formula:

$$\hat{y}_t = (w_1 x_{t-1} + w_2 x_{t-2} + \cdots + w_n x_{t-n}) \\ w_1 + w_2 + \cdots + w_n = 1 \tag{11}$$

where is the weight coefficient, and the sum is 1.

4) ARIMA Method: The ARIMA is based on the ARMA model. The ARIMA model was first proposed by Box and Jenkins in the 1970s and is widely used in the aerospace field [27].

The ARIMA(p, d, q) model is

$$\varphi_p(B)(1 - B)^d Y_t = \theta_q(B)\varepsilon_t \tag{12}$$

Y_t, φ, B, θ, ε, p, d, and q represent the predicted vibration signal, AR model parameters, backward shift operator, MA model parameters, zero-mean white noise, autoregressive term, MA, and number of differences, respectively. The

TABLE I
Comparison of the Three Error Indicators of the Algorithm Prediction Results

Method	LSTM			ARIMA			GRU			LIGHTGBM			WMA		
Index	RMSE	MAPE	R^2	RMSE	MAPE	R^2	RMSE	MAPE	R^2	RMSE	MAPE	R^2	RMSE	MAPE	R^2
Pogo	0.002	0.623	0.535	0.005	0.002	−0.975	0.002	0.001	0.477	0.003	0.001	0.366	0.002	0.0016	0.436
	1.881	243.836	0.695	4.661	1.003	−0.885	1.857	0.365	0.703	2.577	0.365	0.427	2.508	0.367	0.458
	12.061	351.247	0.522	58.204	4.385	10.146	11.034	0.668	0.600	13.422	0.668	0.408	11.444	0.617	0.570
Low-FRE	0.005	19.168	0.992	0.632	0.404	−111.457	0.010	0.006	0.969	0.008	0.006	0.980	0.030	0.009	0.985
	0.0827	14.453	0.199	0.098	0.0433	−0.151	0.056	0.020	0.632	0.082	0.020	0.208	0.070	0.026	0.384
	0.007	3.366	0.397	0.025	0.016	−6.086	0.007	0.005	0.378	0.007	0.005	0.458	0.008	0.006	0.235
High-FRE	0.125	38.464	0.633	0.349	0.168	−1.882	0.125	0.049	0.634	0.120	0.049	0.665	0.142	0.053	0.527
	0.593	131.832	0.564	1.160	0.386	−0.680	0.586	0.168	0.575	0.641	0.168	0.492	0.590	0.167	0.569
Fluctuation	3.362	214.379	0.431	5.337	0.472	−0.129	3.327	0.293	0.567	3.717	0.293	0.459	4.425	0.331	0.230
	2.669	179.791	0.506	4.020	0.714	−0.138	2.464	0.199	0.579	2.924	0.199	0.407	3.024	0.177	0.362
	1.722	324.107	0.709	14.1562	2.800	−18.932	1.671	0.280	0.726	1.824	0.280	0.674	1.865	0.245	0.657
Shock	514.729	28.136	0.847	5942.834	0.883	−18.372	779.443	0.078	0.649	536.688	0.078	0.834	146.726	0.017	0.988
	5.730	119.204	0.644	13.460	0.643	−0.688	5.672	0.397	0.65	5.137	0.397	0.714	5.138	0.410	0.732
Noise	18.948	8.218	−16.553	14.555	0.107	−9.414	3.529	0.007	0.391	1.197	0.007	0.9305	1.923	0.011	0.820
	6.347	2.733	−0.008	10.866	0.075	−0.803	10.047	0.026	-1.526	5.131	0.026	0.341	5.317	0.031	0.463

differential transformation is added to the ARIMA model, which solves the defect that the ARMA model is not suitable for nonstationary sequences.

5) *LightGBM Method:* The gradient boosting decision tree (GBDT) is an estimated model in machine learning. The main idea of GBDT is to use iteratively trained weak classifiers (decision trees) to obtain the optimal model, which has the advantages of a good training effect and is not easily overfit. A light gradient boosting machine (Light-GBM) is a framework for implementing GBDT algorithms that supports efficient parallel training and has the following advantages: faster training speed, lower memory consumption, better accuracy in terms of distributed support, and faster processing of massive data [28].

C. Predicted Results

Six types of signals are predicted based on five methods, and the error of the prediction results is shown in Table I. The prediction effect of the data prediction is shown in Fig. 5.

The R^2 is the degree of model fitting, MAPE is the mean absolute percentage error, and RMSE is the root mean square error, reflecting the prediction accuracy of the algorithm from multiple angles.

According to Table I and Fig. 6, the GRU algorithm has the best prediction effect for longer sequences compared with that of the other types of algorithms experimented on in this article. The LightGBM algorithm has the most balanced prediction effect for long and short sequences. The prediction effect of the weighted MA algorithm and LSTM on long and short series is also relatively balanced. Due to the short sequence length, the ARIMA algorithm has the worst fit and the lowest prediction accuracy in this experiment.

D. Evaluation Set Generation

The evaluation set generation is mainly based on the predicted data waveform not the prediction error. The common method is based on combining the RMSE of the prediction result and the membership function to fuzz and defuse the final result. Fig. 7 shows the commonly used trapezoidal membership degree function.

The abscissa threshold corresponding to multiple types of evaluation indicators is defined according to expert experience: a_1, a_2, a_3, a_4, b_2, b_3, b_4, and b_5. However, this conventional approach is only suitable in situations where the output is difficult to analyze, and the evaluation value is difficult to determine. It is a method of approaching the final evaluation indicator as close as possible when dealing with ambiguity. Under the condition that the data used in this article are no longer ideal, the test data that should be used as the evaluation criterion of the membership function are vague in terms of health status and thus need to be evaluated.
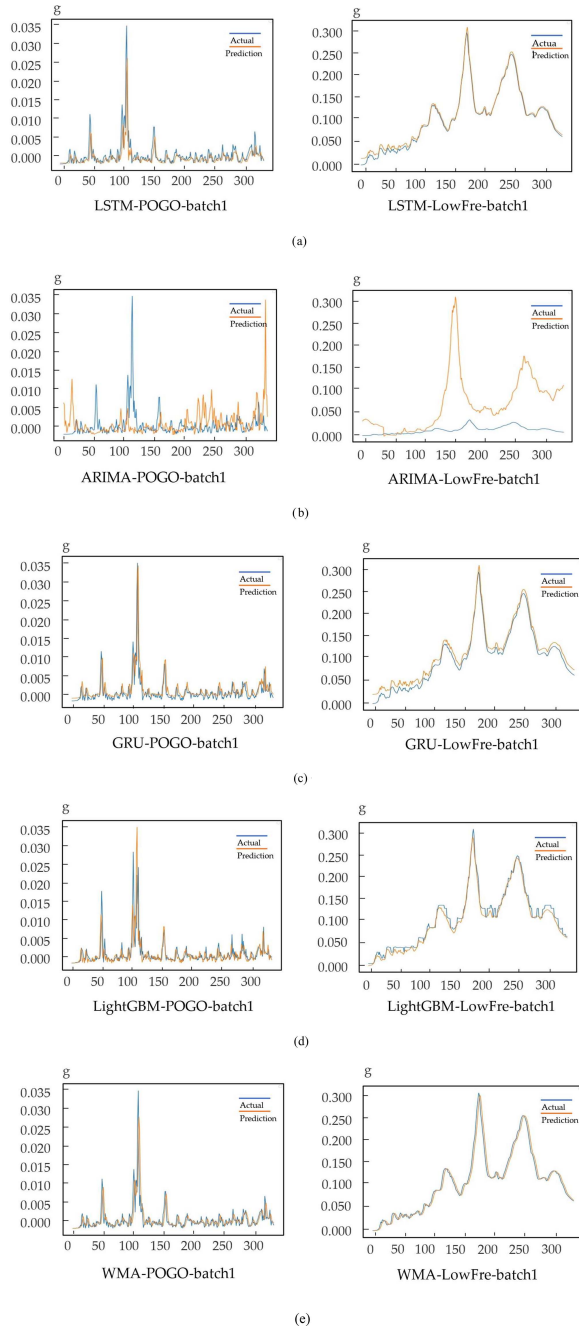
Fig. 6. Prediction examples of five algorithms. The image on the left-hand side is the first batch of pogo vibrations, and the image on the right-hand side is the first batch of low-frequency vibrations. (a) LSTM prediction examples. (b) ARIMA prediction examples. (c) GRU prediction examples. (d) LightGBM prediction examples. (e) WMA prediction examples.

At the same time, the threshold of the membership function is more difficult to grasp, and there is no unified evaluation benchmark for the prediction data.

Therefore, when processing the results of predicting engine vibration signals, a mathematical statistical evaluation matrix generation method is proposed. The specific method is as follows: compare the predicted waveform with the ideal waveform and calculate the probability value of the
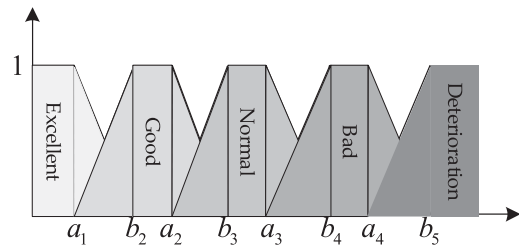

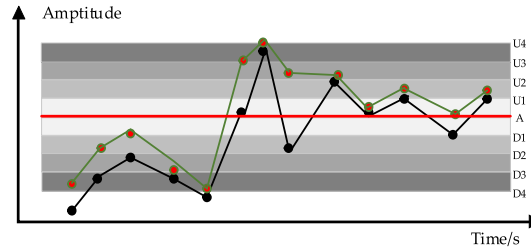Fig. 7. Schematic diagram of the traditional membership function method.

Fig. 8. Evaluation set generation method, where the threshold schematic diagram is divided.

predicted value in each deviation distribution interval as the value of each evaluation index.

The evaluation set generation method in this article mainly combines actual historical rocket launch data and uses the ideal signal state under normal conditions as the benchmark. Ideally, the vibration signal is a stationary signal with small amplitude fluctuations. To simplify the calculation, the fluctuation range is negligible compared to the set threshold.

According to expert experience, a set of healthy comments is excellent, good, normal, bad, and deterioration, corresponding to each color block, as shown in Fig. 8. The red line represents the ideal baseline, the green line represents the forecast wave, and the black line represents the actual wave.

The average waveform amplitude of the signal before the vibration condition occurs is A, the total sampling points of the test data is N, the upper and lower thresholds of the reference waveform are set to U_i and $D_i (0 < i <= 4)$, respectively, and the number of points in each threshold interval is n_i.

The status range is set to $\varphi_j (0 < j <= 5)$, φ_1 stands for excellent status, φ_2 stands for good status, and so on

$$\begin{cases} \varphi_1, A - D_1 < \varphi <= A + U_1 \\ \varphi_2, A + U_1 < \varphi <= A + U_2 || A - D_1 < \varphi <= A - D_2 \\ \varphi_3, A + U_2 < \varphi <= A + U_3 || A - D_2 < \varphi <= A - D_3 \\ \varphi_4, A + U_3 < \varphi <= A + U_4 || A - D_3 < \varphi <= A - D_4 \\ \varphi_5, \varphi < A - D_4 || A + U_4 < \varphi. \end{cases}$$
(13)

Each individual evaluation P in the evaluation set matrix is counted by the state interval of each sampling point of the prediction data, and the percentage is scored according to the interval probability
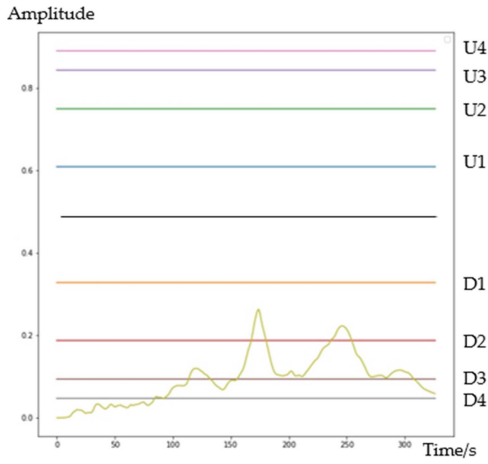
$$P_i = \frac{n_i}{N}.$$
(14)

Fig. 9. First batch vibration signal is shown as an example to divide the threshold.

In the experiment, the predicted waveforms of various signals are predicted, and the real test data and prediction data are compared with the ideal reference state. According to expert experience, the upper and lower thresholds of the four segments are set to 0.3, 0.6, 0.8, and 0.9 times the mean of the first 20% of the real test data, and the deterioration index is the upper and lower limits greater than 0.9 times the mean benchmark. In Fig. 9, a low-frequency vibration acquisition is used as an example.

The black line in the figure is the mean value of 0.4679 in the previous part of the test data, and the yellow line is the predicted waveform. The proportion of sampling points in the range of D_1-U_1 in the predicted waveform is calculated to obtain the excellent evaluation health level.

By counting the proportion of points between U_1-U_2 and D_1-D_2, a good evaluation value can be obtained. The threshold index for deterioration evaluation is $> U_4 \&\& < D_4$. Similarly, the evaluation values of the other health evaluations can be calculated.

The LSTM model is used as an example. The evaluation values of the predicted data and actual data of 15 vibration signal batches of six categories are calculated, and the following evaluation sets are generated. The evaluation error comparison of the actual and predicted data can be completed according to its evaluation matrix. The results of the evaluation are shown in Tables II and III.

E. Prediction Time Analysis

The experimental hardware platform is an i7-11700K CPU and a 3070 GPU with high-performance computing capabilities. The pogo vibration, low-frequency signal, high-frequency signal, and fluctuation are sampled from 50 min of historical data, and approximately 3000 sampling points are used as training data. The shock and noise signals are sampled from 1000 and 500 sampling points, respectively, for training. Under the current algorithm parameter settings, the maximum training and calculation times are approximately 15 s, and according to the proportion of prediction data, the data predicted by the platform are converted into

TABLE II
Evaluation Probability of the Waveform Predicted by the LSTM Method

Evaluation index	Batch	Excellent	Good	Normal	Bad	Deterioration
Pogo	1	0.202	0.325	0.104	0.044	0.325
	2	0.372	0.310	0.063	0.050	0.205
	3	0.211	0.259	0.290	0.158	0.082
Low-FRE	1	0.000	0.065	0.265	0.369	0.302
	2	0.570	0.157	0.006	0.009	0.258
	3	0.357	0.369	0.268	0.000	0.007
High-FRE	1	0.085	0.233	0.640	0.035	0.007
	2	0.259	0.328	0.233	0.057	0.123
Fluctuation	1	0.242	0.375	0.240	0.058	0.085
	2	0.025	0.038	0.079	0.505	0.353
	3	0.063	0.110	0.073	0.101	0.653
Shock	1	0.000	0.000	0.000	0.000	1.000
	2	0.231	0.264	0.223	0.066	0.216
Noise	1	1.000	0.000	0.000	0.000	0.000
	2	1.000	0.000	0.000	0.000	0.000

TABLE III
Evaluation Probability of the Actual Waveform

Evaluation index	Batch	Excellent	Good	Normal	Bad	Deterioration
Pogo	1	0.312	0.281	0.117	0.038	0.252
	2	0.303	0.233	0.139	0.054	0.271
	3	0.233	0.274	0.221	0.104	0.167
Low-FRE	1	0.000	0.092	0.437	0.218	0.252
	2	0.428	0.169	0.083	0.108	0.212
	3	0.209	0.255	0.209	0.074	0.252
High-FRE	1	0.082	0.145	0.539	0.205	0.028
	2	0.211	0.290	0.202	0.088	0.208
Fluctuation	1	0.259	0.344	0.230	0.047	0.120
	2	0.025	0.041	0.091	0.322	0.521
	3	0.063	0.104	0.091	0.120	0.621
Shock	1	0.000	0.000	0.000	0.000	1.000
	2	0.190	0.289	0.190	0.074	0.256
Noise	1	1.000	0.000	0.000	0.000	0.000
	2	1.000	0.000	0.000	0.000	0.000

a regular collection time of approximately 5 min, which shows that the platform can achieve good results in terms of prediction timeliness.

IV. MULTILAYER WEIGHT GENERATION

The types and sources of launch vehicle engine vibration signals are difficult to locate for specific components, and the impact of different vibration types on the normal flight of a launch vehicle is different. The data reliability and effectiveness of different sensors cannot be equal. Converting the degree of impact into percentage weights under a uniform measure is necessary for assessing a vehicle's state of health.

A. Analytic Hierarchy Method

For the health value assessment of a launch vehicle engine system, a quantitative analysis of multiple conditions and factors is needed. The electrical environment inside a launch vehicle engine is a typical giant system and a fuzzy environment. Therefore, it is impossible to grasp the weight of each factor in the system by relying on human experience under the same weight standard. Based on historical data and the summary of past failure modes, experts can obtain the weight relationship between two factors, that is, the impact of factor A on the entire system is quantified relative to that of factor B, but when there are many factors involved, experts cannot directly obtain a multilevel, multifactor influence weight relationship.

Considering the hierarchical complexity of system equipment, a multilayer multifactor weight matrix is generated based on the analytic hierarchy process (AHP) method. The AHP method was first proposed by American scientist T. L. Saaty in the 1970s [29] and has been applied to network system theory and multiobjective comprehensive evaluation. It mainly solves the decision-making problems of interrelated and mutually restricting complex systems and is widely used in aerospace, electrical, operations research, and other fields.

When using the AHP to construct a rocket engine vibration signal model and obtain the weights of each type of factor, the method is roughly divided into the following steps:

1) Establish a hierarchical model according to the type and batch of launch vehicle engine vibration signals.
2) Based on historical statistics and expert experience, construct a judgment matrix according to the weight relationship between factors at the same level, also known as reciprocal matrices.

$$A_{ij} = \begin{pmatrix} a_{11} & \cdots & a_{1j} \\ \vdots & \ddots & \vdots \\ a_{n1} & \cdots & a_{nn} \end{pmatrix}, a_{ij} > 0, a_{ij} \times a_{ji} = 1. \tag{15}$$

3) Calculate the maximum eigen root λ_{max} and eigenvector ω of the reciprocal matrix according to the criteria $A_{ij}\omega = \lambda_\omega$ to facilitate subsequent calculation.
4) Normalize the feature vectors and calculate the weight values of all elements contained in each layer separately. The weight calculation formula is as follows:

$$W_k = \sum_{j=1}^{n} a_{kn} \bigg/ \sum_{i=1}^{n} \sum_{j=1}^{n} a_{ij}. \tag{16}$$

5) Conduct a consistency test on the matrix. The credibility of the manually determined matrix is tested. If there is a contradiction between the two weights of the elements, the consistency test is not passed, the credibility of the result of introducing the artificial weighted positive and negative matrix is increased,
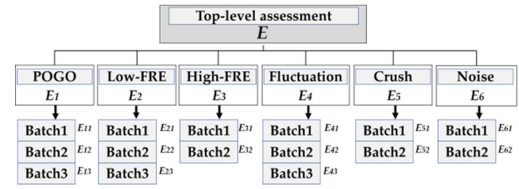

Fig. 10. Symbolic representation of each factor in the weight set generation method.

and the consistency index is as follows:

$$CI = \frac{\lambda_{max} - n}{n - 1} \quad (n > 1) . \tag{17}$$

The corresponding immediate mean agreement metric $RI = 0.52$, so the consistency ratio (CR) is

$$CR = \frac{CI}{RI}. \tag{18}$$

When $CR < 0.1$, the consistency test is considered to be passed, and n is the established system-level order.

6) Generate subjective weight vectors.

B. Weight Generation

The corresponding table of consistency indicators is shown in Table IV.

The system weight allocation architecture in this article is shown in Fig. 10. The overall system is summarized as follows: $E = \{E_1, E_2, E_3, E_4, E_5, E_6\}$, where E_1, E_2, E_3, E_4, E_5, and E_6 represent pogo vibration, low-frequency vibration, high-frequency vibration, fluctuation, shock, noise in order. We can see in the figure that the overall system is divided into three levels, so n is 3. The overall hierarchy of the vibration signal of the ascent launch vehicle engine is divided into three stages, in which the subtarget layer contains a weight vector: $W(E_1, E_2, E_3, E_4, E_5, E_6)$. The factor layer consists of the following six weight vectors: $W_1(E_{11}, E_{12}, E_{13})$, $W_2(E_{21}, E_{22}, E_{23})$, $W_3(E_{31}, E_{32})$, $W_4(E_{41}, E_{42}, E_{43})$, $W_5(E_{51}, E_{52})$, and $W_6(E_{61}, E_{62})$.

The multilevel reciprocal matrix provided by the China Academy of Launch Vehicle Technology is shown in Table V. Due to space limitations, only the reciprocal matrix of the subtarget layer and a set of factor layers are shown.

The reciprocal matrix, such as that for the low-frequency vibration, is given in the same way, as shown in Table VI. According to the AHP method in Section IV-A, the subtarget layer weight is $W = (0.33, 0.20, 0.07, 0.27, 0.10, 0.03)$, and the maximum eigenvalue is 6.003449. Therefore, $CR = 0.000507$, and the consistency test is passed. The weight vectors of each factor under the six types of subgoals are given as follows:

$W_1 = (0.14, 0.29, 0.57)$
$W_2 = (0.14, 0.29, 0.57)$
$W_3 = (0.33, 0.67)$
$W_4 = (0.14, 0.29, 0.57)$
$W_5 = (0.33, 0.67)$
$W_6 = (0.33, 0.67)$.

TABLE IV
Consistency Test Random Indicators (RIs)

Order	1	2	3	4	5	6	7	8	9	10	11	…
RI	0	0	0.52	0.89	1.12	1.24	1.36	1.41	1.46	1.49	1.52	…

TABLE V
Reciprocal Matrix of the Subtarget Layer

	Pogo	Low-FRE	High-FRE	Fluctuation	Shock	Noise
Pogo	1	3/2	5	4/3	3	9
Low-FRE	2/3	1	3	3/4	2	6
High-FRE	1/5	1/3	1	1/4	2/3	2
Fluctuation	3/4	3/4	4	1	8/3	8
Shock	1/3	1/2	3/2	3/8	1	3
Noise	1/9	1/6	1/2	1/8	1/3	1

TABLE VI
Reciprocal Matrix of the Low-Frequency Signal

Sensor Batch	1	2	3
1	1	1/2	1/4
2	2	1	1/2
3	4	2	1

TABLE VII
Health Evaluation Values and Evaluation Errors for Five Kinds of Algorithms

Method	LSTM	ARIMA	GRU	LightGBM	WMA
Evaluation Value	57.61	58.59	61.65	57.56	61.56
Error (%)	3.71	2.73	0.33	3.76	0.24

After testing, the results of six groups of consistency tests passed. The weight experiment results show that pogo vibration, fluctuation, and low-frequency vibration have the greatest influence on the health state of the ascent section of the launch vehicle engine in the subtarget layer. At the same time, according to expert experience, the data after the sensor batch can better reflect the authenticity and real time of the state, so the weight is also higher, and the results are in line with the experience expectations.

V. FUZZY COMPREHENSIVE ASSESSMENT

A. Principles and Steps of Fuzzy Comprehensive Assessment

The fuzzy comprehensive evaluation method has the advantages of clear results and strong systematization and is thus suitable for a more comprehensive and in-depth evaluation of multilevel and multifactor objects in a fuzzy environment. A large number of expert systems used in spacecraft health management use historical experience to build a knowledge base and make system evaluation more intelligent through extrapolation, mapping, and other methods. However, in fact, the unstable working conditions of the launch vehicle engine have a great relationship with the launch environment and flight trajectory. At the same time, the frequent iterations of launch vehicle engine technology have not led to the rapid replenishment of the expert system knowledge base. Therefore, the evaluation method based on the expert system is not universal, accurate, or comprehensive.

The evaluation steps of the fuzzy integrated assessment method are as follows:

1) Establish the overall structure of the research objectives and create a multilevel structure to facilitate the subsequent bottom-up evaluation.
2) Create a collection of comments: $M = m_1, m_2 \cdots m_n$ based on the actual object.
3) Obtain the weight matrix W of the factors in each level and the evaluation matrix V of the underlying signal.
4) Perform fuzzy evaluation operations to obtain the fuzzy evaluation vector of the target layer: $B = V \cdot W$.
5) According to the needs of the project, assign the scores that can be obtained for each type of evaluation and generate a score vector: F.
6) Obtain the statistical health score, which is the health of the system.

B. Scoring Rocket Engine Health Based on Fuzzy Comprehensive Assessment

From Sections III and IV, we have obtained the evaluation matrix $V = v_1, v_2 \cdots v_{15}$ and the weight matrix $W = w, w_1, w_2, \cdots w_6$. v_i represents the single evaluation vector of the underlying factor layer, w represents the subtarget layer weight vector, and w_i represents the weight vector for each type of vibration signal.

From Section III, the comment collection is set to $M =$ {excellent, good, normal, bad, deterioration}, and the score set is set to $F = (1.0, 0.8, 0.6, 0.4, 0.1)$. Therefore, the health evaluation vector of the target layer-launch vehicle engine system under the multiaccumulation vibration signal is shown below:

$$B_1 = V_1 \cdot W = (0.238, 0.219, 0.171, 0.113, 0.259)$$
$$B_2 = V_2 \cdot W = (0.213, 0.197, 0.166, 0.107, 0.318)$$
$$B_3 = V_3 \cdot W = (0.195, 0.227, 0.185, 0.099, 0.294)$$
$$B_4 = V_4 \cdot W = (0.239, 0.229, 0.164, 0.112, 0.256)$$
$$B_5 = V_5 \cdot W = (0.212, 0.197, 0.166, 0.107, 0.319)$$
$$B_6 = V_6 \cdot W = (0.246, 0.222, 0.170, 0.080, 0.303).$$

The health score calculation formula is $B \cdot F$, the real data health score is 61.32, the prediction evaluation result is shown in the table, and the minimum error is 0.24%. The status is in line with expert experience.

VI. CONCLUSION

This article proposes a predictive evaluation method for launch vehicle health management systems. This method has the advantages of objectivity, high precision, and strong versatility. In the experiment in this article, the actual data were used to verify that the proposed method has high accuracy. The method has important guiding significance for the health prediction management of vibration signals of launch vehicles in the ascent section and can be used for the formulation of rocket launch and flight strategies.

However, in the actual project, our work still has the following shortcomings:

1) The accuracy of the evaluation depends on the accuracy of the prediction algorithm and the effectiveness of the evaluation depends on the speed of the prediction algorithm.
2) The method ignores the association rules between vibration categories.
3) Our work ignores the variation in weights under different operating conditions of rockets.

Based on the above shortcomings, future work can be as follows:

1) A specific prediction algorithm to optimize the prediction accuracy when the prediction speed reaches the target can be designed.
2) The association rules between vibration categories, and the influence of the weight relationship through the association rules can be considered.
3) Data recognition and classification algorithms can be applied to incorporate an weight adaptive module.

REFERENCES

[1] C. Zhang, X. T. Rui, B. Rong, and G. P. Wang, "Vibration characteristics of airborne multiple launch rocket systems," *J. Vib. Eng.*, vol. 26, no. 1, pp. 15–19, Feb. 2013, doi: 10.16385/j.cnki.issn.1004-4523.2013.01.018.

[2] J. Cha et al., "Fault detection and diagnosis algorithms for transient state of an open-cycle liquid rocket engine using nonlinear Kalman filter methods," *Acta Astronautica*, vol. 163, pp. 147–156, Oct. 2019, doi: 10.1016/j.actaastro.2019.03.075.

[3] G. Leng, T. M. McGinnity, and G. Prasad, "An approach for online extraction of fuzzy rules using a self-organising fuzzy neural network," *Fuzzy Sets Syst.*, vol. 150, no. 2, pp. 211–243, Mar. 2005, doi: 10.1016/j.fss.2004.03.001.

[4] D. Ge and X.-J. Zeng, "A self-evolving fuzzy system which learns dynamic threshold parameter by itself," *IEEE Trans. Fuzzy Syst.*, vol. 27, no. 8, pp. 1625–1637, Aug. 2019, doi: 10.1109/TFUZZ.2018.2886154.

[5] K. Subramanian, S. Suresh, and N. Sundararajan, "A metacognitive neuro-fuzzy inference system (McFIS) for sequential classification problems," *IEEE Trans. Fuzzy Syst.*, vol. 21, no. 6, pp. 1080–1095, Dec. 2013, doi: 10.1109/TFUZZ.2013.2242894.

[6] Z. Z. Zhang et al., "Review on fault diagnosis technology of liquid rocket engine," *J. Propulsion Technol.*, vol. 43, no. 6, p. 43, Jun. 2022, doi: 10.13675/j.cnki.tjjs.210345.

[7] M. Davidson and J. Stephens, "Advanced health management system for the space shuttle main engine," in *Proc. 40th Amer. Inst. Aeronaut. Astronaut./Amer. Soc. Mech. Engineers/Soc. Autom. Engineers/ASEE Joint Propulsion Conf. Exhib.*, 2004, Art. no. 3912.

[8] L. A. Breedveld, *A Comparative Evaluation of Models and Algorithms in Model-Based Fault Diagnosis*. Delft, The Netherlands: Delft Univ. Technol., 2004.

[9] A. N. Srivastava and W. Buntine, "Predicting engine parameters using the optic spectrum of the space shuttle main engine exhaust plume," in *Proc. 10th Comput. Aerosp. Conf.*, 1995, p. 954.

[10] M. W. Hawman et al., "Framework for a space shuttle main engine health monitoring system," NASA Contractor Rep. NASA-CR-185224, Washington,DC, USA, 1990.

[11] T. Yairi, N. Takeishi, T. Oda, Y. Nakajima, N. Nishimura, and N. Takata, "A data-driven health monitoring method for satellite housekeeping data based on probabilistic clustering and dimensionality reduction," *IEEE Trans. Aerosp. Electron. Syst.*, vol. 53, no. 3, pp. 1384–1401, Jun. 2017, doi: 10.1109/TAES.2017.2671247.

[12] J. Engle, B. Don, and M. John, "Prelaunch expert system for space shuttle propulsion system health monitoring," in *Proc. 26th Joint Propulsion Conf.*, 1990, Art. no. 1888.

[13] J. Kurien and P. P. Nayak, "Back to the future for consistency-based trajectory tracking," in *Proc. Assoc. Advance. Artif. Intell./Int. Assoc. Arson Investigators*, 2000, pp. 370–371.

[14] J. G. Perry et al., "An expert system approach to turbopump health monitoring," in *Proc. 24th Joint Propulsion Conf.*, 1988, Art. no. 3117.

[15] L. Xu, S. Zhao, N. Li, Q. Gao, T. Wang, and W. Xue, "Application of QGA-BP for fault detection of liquid rocket engines," *IEEE Trans. Aerosp. Electron. Syst.*, vol. 55, no. 5, pp. 2464–2472, Oct. 2019, doi: 10.1109/TAES.2018.2890352.

[16] N. Aiswarya, S. S. Priyadharsini, and K. S. Moni, "An efficient approach for the diagnosis of faults in turbo pump of liquid rocket engine by employing FFT and time-domain features," *Australian J. Mech. Eng.*, vol. 16, no. 3, pp. 163–172, Dec. 2018, doi: 10.1080/14484846.2016.1264285.

[17] Y. Y. Wu, N. G. Li, W. Xue, and L. Xu, "Fault diagnosis of liquid-propellant rocket engines base on improved PSO to optimize LSSVM," *Comput. Simul.*, vol. 37, no. 5, pp. 49–54, May 2020.

[18] B. Wang, Y. Lei, N. Li, and T. Yan, "Deep separable convolutional network for remaining useful life prediction of machinery," *Mech. Syst. Signal Process.*, vol. 134, Dec. 2019, Art. no. 106330, doi: 10.1016/j.ymssp.2019.106330.

[19] H. Miao, B. Li, C. Sun, and J. Liu, "Joint learning of degradation assessment and RUL prediction for aeroengines via dual-task deep LSTM networks," *IEEE Trans. Ind. Inform.*, vol. 15, no. 9, pp. 5023–5032, Sep. 2019, doi: 10.1109/TII.2019.2900295.

[20] F. Tao et al., "Digital twin driven prognostics and health management for complex equipment," *Cirp Ann.*, vol. 67, no. 1, pp. 169–172, 2018, doi: 10.1016/j.cirp.2018.04.055.

[21] X. G. Zhou and B. Sun, "Stability analysis of POGO vibration considering multiple parameter variations," *Manned Spaceflight*, vol. 25, no. 3, pp. 367–371, Jun. 2019, doi: 10.16329/j.cnki.zrht.2019.03.013.

[22] Y. Yang, T. Yu, Y. N. Guo, Z. J. Jia, and Y. P. Wang, "Application of fluctuating pressure measurement technology in rocket engine test," *J. Astronaut.*, vol. 42, no. 7, pp. 917–926, Jul. 2021, doi: 10.3873/j.issn.1000-1328.2021.07.012.

[23] H. Guo, X. Lin, and K. Zhu, "Pyramid LSTM network for tool condition monitoring," *IEEE Trans. Instrum. Meas.*, vol. 71, 2022, Art. no. 2509511, doi: 10.1109/TIM.2022.3173278.

[24] X. Hong et al., "Predicting Alzheimer's disease using LSTM," *IEEE Access*, vol. 7, pp. 80893–80901, 2019, doi: 10.1109/ACCESS.2019.2919385.

[25] Y. Li, Y. Yang, K. Zhu, and J. Zhang, "Clothing sale forecasting by a composite GRU-prophet model with an attention mechanism," *IEEE Trans. Ind. Inform.*, vol. 17, no. 12, pp. 8335–8344, Dec. 2021, doi: 10.1109/TII.2021.3057922.

[26] Y. Zhao, X. He, D. Zhou, and M. G. Pecht, "Detection and isolation of wheelset intermittent over-creeps for electric multiple units based on a weighted moving average technique," *IEEE Trans. Intell. Transp. Syst.*, vol. 23, no. 4, pp. 3392–3405, Apr. 2022, doi: 10.1109/TITS.2020.3036102.

[27] G. Box and G. M. Jenkins, "Time series analysis, forecasting and control," *J. Roy. Statist. Soc. Ser. A*, vol. 134, no. 3, 1976.

[28] Z. Mao, M. Xia, B. Jiang, D. Xu, and P. Shi, "Incipient fault diagnosis for high-speed train traction systems via stacked generalization," *IEEE Trans. Cybern.*, vol. 52, no. 8, pp. 7652–7633, Aug. 2022, doi: 10.1109/TCYB.2020.3034929.

[29] T. L. Saaty, "A scaling method for priorities in hierarchical structures," *J. Math. Psychol.*, vol. 15, no. 3, pp. 234–281, Jun. 1977, doi: 10.1016/0022-2496(77)90033-5.

Lijing Huang received the bachelor's degree in electronic science and technology from Hebei University of Technology, Tianjin, China, in 2020. He received the master's degree from the Beijing Institute of Technology, Beijing, China.

His research interests include launch vehicle PHM, artificial intelligence and hardware development.

Zhiguo Zhou (Member, IEEE) received the bachelor's degree in measurement and control technology and instrumentation from Huazhong University of Science and Technology, Wuhan, China, in 1998 and the master's and Ph.D. degrees from Beijing Institute of Technology, Beijing, China, in 2004 and 2009, respectively.

Since 2018, he has been an Associate Professor with the School of Integrated Circuits and Electronics, Beijing Institute of Technology. His main research interests include spacecraft fault diagnosis, image processing and signal, and image processing.

Ruliang Lin received the bachelor's and master's degrees from Beijing Institute of Technology, Beijing, China, in 2007 and 2009, respectively.

His research interests include fault diagnosis, command and control and information security of launch vehicles.